AGU PUBLICATIONS

Geophysical Research Letters

RESEARCH LETTER
10.1002/2014GL063020

Key Points:
- Define a new parameter to describe the earthquake size
- Introduce borehole data to earthquake early warning
- The proposed earthquake size is related to the strong ground motion

Correspondence to:
T.-L. Lin,
mulas62@gmail.com

Citation:
Huang, P.-L., T.-L. Lin, and Y.-M. Wu (2015), Application of τ_c*P*d* in earthquake early warning, *Geophys. Res. Lett.*, *42*, 1403–1410, doi:10.1002/2014GL063020.

Received 31 DEC 2014
Accepted 12 FEB 2015
Accepted article online 15 FEB 2015
Published online 13 MAR 2015

Application of τ_c*P*d* in earthquake early warning

Po-Lun Huang[1], Ting-Li Lin[1], and Yih-Min Wu[2]

[1]Department of Earth Sciences, National Cheng Kung University, Tainan, Taiwan, [2]Department of Geosciences, National Taiwan University, Taipei, Taiwan

Abstract Rapid assessment of damage potential and size of an earthquake at the station is highly demanded for onsite earthquake early warning. We study the application of τ_c*P*d* for its estimation on the earthquake size using 123 events recorded by the borehole stations of KiK-net in Japan. The new type of earthquake size determined by τ_c*P*d* is more related to the damage potential. We find that τ_c*P*d* provides another parameter to measure the size of earthquake and the threshold to warn strong ground motion.

1. Introduction

Over decades of development, earthquake early warning (EEW) system is proven to be one of the effective tools for real-time seismic hazard mitigation and has been developed and operated in many countries, for example, Italy, Japan, Mexico, Taiwan, and the Southern California [*Kanamori et al.*, 1997; *Allen et al.*, 2009; *Lee and Wu*, 2009; *Zollo et al.*, 2010; *Satriano et al.*, 2011]. EEW aims to provide timely alerts before the destructive ground shakings strike protected targets, sensitive facilities, or public transportations.

The two main types of EEW systems are mostly adopted, regional and onsite warning systems. In regional warning, the seismic data from seismic sensors or arrays deployed in the source region are used to predict the strong ground motions at a more distant region. In onsite warning, the initial *P* wave motion of a single station or an array is used to predict the peak ground motion of later arriving *S* and surface waves, which commonly have higher amplitudes or destructive energy than that of the initial *P* wave at the same site. Generally, the regional warning has a higher accuracy than the onsite one because of the use of more stations and complete source rupturing. On the other hand, the onsite warning has a shorter reporting time than the regional one.

The average period (τ_c) of vertical displacement from the first 3 s of the *P* wave is proven to have an acceptable correlation with the size of an earthquake [*Kanamori*, 2005; *Wu and Kanamori*, 2005a; *Wu et al.*, 2007; *Wu and Kanamori*, 2008a, 2008b]. The peak amplitude of displacement (P*d*) [*Wu et al.*, 2007; *Wu and Kanamori*, 2008a, 2008b, 2005b; *Zollo et al.*, 2006] of vertical displacement in the first several seconds after the arrival of the *P* wave reflects the attenuation relationship with distance as a function of magnitude and is also well correlated with the peak ground velocity (PGV).

In order to improve the reliability, *Wu and Kanamori* [2005b] proposed that the value of τ_c*P*d* = 1.0 s cm is a good single indicator for identifying damaging earthquakes in Taiwan. *Alick et al.* [2011] consistently observed that the product of τ_c*P*d* is a good threshold for detecting damaging earthquakes in Turkey. Therefore, the value of τ_c*P*d* could be used in the onsite warning as a threshold value for damaging earthquakes. However, the events used in their studies are not plenty. *Wu and Kanamori* [2005b] studied a total of 26 events, including of five damaging events. *Alick et al.* [2011] collected two damaging events out of a total of 12 events. In this study, we used 123 events (Figure 1a) recorded by the KiK-net (Figure 1b) to study the application of the value of τ_c*P*d*.

2. Seismic Network and Data

In this study, we acquired the borehole strong-motion data from the KiK-net stations of the National Research Institute for Earth Science and Disaster Prevention, Japan (NIED) [*Aoi et al.*, 2011] to compute τ_c and P*d*. KiK-net is a strong-motion seismograph network, which consists of approximately 700 locations nationwide. Each KiK-net station has strong-motion seismographs installed both on the ground surface and at the bottom

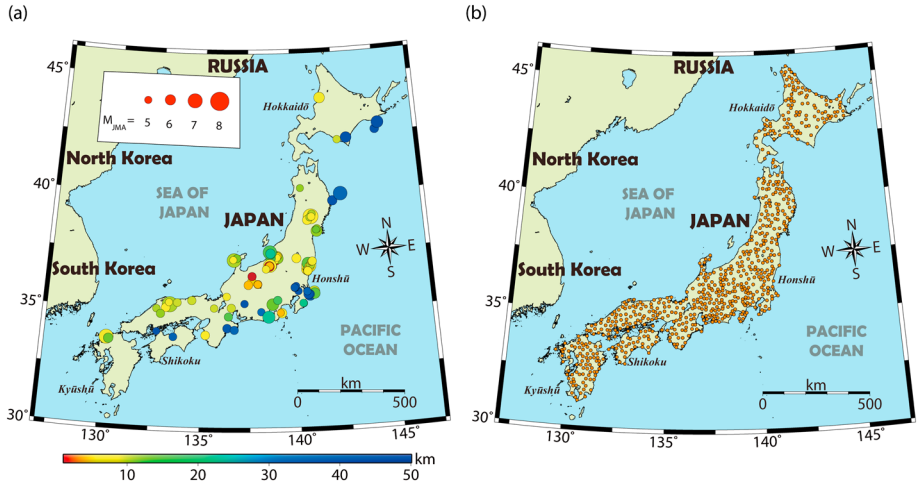

Figure 1. (a) The epicenter locations of the 123 events used in this study with the color indicates the focal depth. (b) The station distribution of the KiK-net network.

of the boreholes of 100 m or more in depth. In this study, we only used the borehole data in order to reduce the receiver site near-surface effects and to better extract the source signature registered on the initial portion after *P* wave arrival.

We selected 123 inland and offshore (distance to shoreline < 10 km) regional earthquakes from the KiK-net catalog occurred between 1996 and 2012 with $M_{JMA} > 5.0$ and the focal depths shallower than 50 km

Table 1. Event Information

Origin	Time	Latitude (N)	Longitude (E)	Depth (km)	Magnitude (M_{JMA})	Nsta[a] (stations)	Hypocentral Distance (km)
1998/04/22	20:32	35.17	136.56	10	5.4	18	24.98
1998/08/16	03:31	36.32	137.63	5	5.4	13	40.01
2000/10/06	13:30	35.28	133.35	11	7.3	220	13.13
2000/10/08	13:17	35.14	133.15	8	5.5	75	13.70
2000/10/08	20:51	35.37	133.31	9	5	57	22.61
2000/10/31	01:43	34.29	136.34	44	5.5	118	49.96
2001/01/04	13:18	36.96	138.76	14	5.1	105	17.84
2001/01/12	08:00	35.47	134.49	10	5.4	129	25.10
2001/03/26	05:41	34.11	132.72	49	5	89	53.40
2001/04/03	23:57	35	138.11	33	5.1	73	54.90
2001/08/25	22:21	35.15	135.66	10	5.1	98	19.21
2002/09/16	10:10	35.37	133.74	10	5.3	119	10.09
2003/05/12	00:57	35.87	140.08	47	5.2	120	45.79
2003/05/17	23:33	35.74	140.65	47	5.1	86	49.04
2003/07/26	00:13	38.43	141.16	12	5.5	140	22.71
2003/07/26	07:13	38.4	141.17	12	6.2	193	25.37
2003/07/26	16:56	38.5	141.19	12	5.3	121	18.70
2003/07/28	04:08	38.46	141.15	14	5	95	21.40
2003/09/28	09:23	42.6	144.81	48	5.5	54	51.49
2004/01/06	14:50	34.22	136.71	37	5.4	130	38.36
2004/06/11	03:12	42.32	143.13	48	5.2	92	51.69
2004/08/10	15:13	39.67	142.13	48	5.8	142	52.32
2004/10/08	04:26	42.34	143.12	50	5.1	67	52.82
2004/10/23	17:56	37.29	138.87	13	6.8	286	18.13
2004/10/23	17:59	37.31	138.85	16	5.3	84	92.14
2004/10/23	18:03	37.35	138.98	9	6.3	216	14.79
2004/10/23	18:07	37.35	138.86	15	5.7	124	17.51
2004/10/23	18:12	37.25	138.83	12	6	202	16.72
2004/10/23	18:34	37.31	138.93	14	6.5	264	17.37

Table 1. (continued)

Origin	Time	Latitude (N)	Longitude (E)	Depth (km)	Magnitude (M_{JMA})	Nsta[a] (stations)	Hypocentral Distance (km)
2004/10/23	18:36	37.26	138.94	7	5.1	68	20.83
2004/10/23	18:57	37.21	138.86	8	5.3	111	13.33
2004/10/23	19:36	37.22	138.82	11	5.3	117	13.91
2004/10/23	19:46	37.3	138.87	12	5.7	168	17.22
2004/10/23	21:44	37.27	138.94	15	5	79	16.28
2004/10/23	23:34	37.32	138.9	20	5.3	133	23.49
2004/10/24	14:21	37.25	138.82	11	5	61	17.90
2004/10/24	23:00	37.18	138.95	2	5.1	25	14.49
2004/10/25	00:28	37.2	138.87	10	5.3	120	22.33
2004/10/25	06:05	37.33	138.95	15	5.8	167	19.22
2004/10/27	10:40	37.29	139.03	12	6.1	226	14.81
2004/11/01	04:35	37.21	138.9	8	5	108	10.91
2004/11/04	08:57	37.43	138.91	18	5.2	121	18.15
2004/11/08	11:32	37.39	139.05	6	5.1	103	15.83
2004/11/10	03:43	37.37	139	5	5.3	100	12.81
2004/12/14	14:56	44.08	141.7	9	6.1	97	12.66
2004/12/28	18:30	37.32	138.98	8	5	79	13.45
2005/01/18	23:09	42.88	145	50	6.4	185	62.58
2005/02/16	04:46	36.03	139.9	45	5.4	135	45.71
2005/03/20	10:53	33.74	130.18	9	7	265	37.33
2005/04/20	06:11	33.68	130.29	14	5.8	131	30.98
2005/06/20	13:03	37.23	138.59	15	5	69	21.17
2005/08/21	11:29	37.3	138.71	17	5	111	22.13
2005/10/16	16:05	36.04	139.94	47	5.1	103	52.69
2006/04/21	02:50	34.94	139.19	7	5.8	107	12.13
2007/03/25	09:42	37.22	136.69	11	6.9	334	37.09
2007/03/25	18:11	37.3	136.84	13	5.3	83	19.56
2007/04/15	12:19	34.79	136.41	16	5.4	161	16.36
2007/04/26	09:03	33.89	133.58	39	5.3	126	39.80
2007/06/11	03:45	37.24	136.65	7	5	48	10.75
2007/07/16	10:13	37.56	138.61	17	6.8	305	33.27
2007/07/16	15:37	37.5	138.64	23	5.8	182	32.66
2007/08/18	16:55	35.34	140.34	20	5.2	49	25.87
2008/06/14	08:43	39.03	140.88	8	7.2	325	8.51
2008/06/14	09:20	38.88	140.68	6	5.7	117	6.95
2008/06/14	12:27	39.14	140.94	11	5.2	89	14.00
2008/06/16	23:14	39	140.84	11	5.3	112	11.40
2009/02/18	06:47	35.66	136.31	9	5.2	172	14.46
2009/08/11	05:07	34.78	138.5	23	6.5	310	31.01
2009/12/17	23:45	34.96	139.13	4	5	66	6.06
2009/12/18	08:45	34.96	139.13	4	5	66	6.38
2010/07/04	04:33	39.02	140.91	7	5.2	103	12.04
2010/09/29	17:00	37.28	140.03	8	5.7	129	16.26
2011/02/27	02:19	36.16	137.46	4	5	104	12.54
2011/02/27	05:38	36.16	137.45	4	5.5	150	12.83
2011/03/12	03:59	36.98	138.6	8	6.7	252	18.28
2011/03/12	04:32	36.95	138.57	1	5.9	178	12.50
2011/03/12	05:42	36.97	138.59	4	5.3	51	15.60
2011/03/15	22:31	35.31	138.71	14	6.4	259	22.49
2011/03/16	12:52	35.84	140.91	10	6.1	213	16.60
2011/03/19	08:49	36.8	140.7	10	5.3	79	15.25
2011/03/19	18:56	36.78	140.57	5	6.1	246	5.60
2011/03/23	07:12	37.08	140.79	8	6	184	19.14
2011/03/23	07:36	37.06	140.77	7	5.8	185	19.49
2011/04/01	19:49	40.26	140.36	12	5	82	14.64
2011/04/11	17:16	36.95	140.67	6	7	357	19.81
2011/04/11	17:26	37.06	140.62	5	5.4	104	40.19
2011/04/11	18:05	36.99	140.73	12	5.1	130	29.96
2011/04/11	20:42	36.97	140.63	11	5.9	216	24.79
2011/04/12	00:57	37.06	140.65	11	5	82	22.64

Table 1. (continued)

Origin	Time	Latitude (N)	Longitude (E)	Depth (km)	Magnitude (M_{JMA})	Nsta[a] (stations)	Hypocentral Distance (km)
2011/04/12	14:07	37.05	140.64	15	6.4	253	16.07
2011/04/13	10:08	36.91	140.71	5	5.7	149	24.79
2011/04/14	07:35	36.78	140.57	9	5.1	79	18.56
2011/04/14	12:09	36.98	140.77	11	5.4	111	9.61
2011/04/21	22:37	35.67	140.69	46	6	183	21.25
2011/04/26	21:12	36.09	139.97	46	5	124	47.62
2011/05/06	02:04	37.1	140.81	6	5.2	53	45.23
2011/05/22	07:06	35.73	140.64	48	5.5	128	17.48
2011/05/25	05:36	37.11	140.83	7	5	37	49.06
2011/06/04	01:57	35.09	132.67	11	5.2	102	17.11
2011/06/23	06:51	39.95	142.59	36	6.9	295	16.88
2011/06/30	08:16	36.19	137.95	4	5.4	111	72.16
2011/06/30	08:21	36.19	137.95	4	5.1	60	9.05
2011/07/05	19:18	33.99	135.23	7	5.5	159	9.05
2011/09/07	22:29	42.26	142.59	10	5.1	51	7.30
2011/09/21	22:30	36.74	140.58	9	5.2	143	23.64
2011/09/23	17:15	36.69	140.62	4	5.1	79	10.80
2011/09/29	19:05	37.13	140.87	9	5.4	118	7.44
2011/10/05	19:00	36.53	137.65	1	5.4	65	17.29
2011/11/20	10:23	36.71	140.59	9	5.3	125	15.59
2011/11/21	19:16	34.87	132.89	12	5.4	128	10.05
2011/12/03	05:55	35.35	140.32	22	5.2	96	13.21
2011/12/14	13:01	35.35	137.24	49	5.1	163	29.25
2012/01/28	07:43	35.49	138.98	18	5.4	163	51.58
2012/02/19	14:54	36.75	140.59	7	5.2	122	18.96
2012/03/10	02:25	36.72	140.61	7	5.4	147	9.05
2012/03/14	21:05	35.75	140.93	15	6.1	213	9.60
2012/04/25	05:22	35.72	140.68	43	5.5	150	17.57
2012/04/29	19:28	35.72	140.6	48	5.8	168	43.99
2012/06/01	17:48	36.03	139.88	44	5.1	158	48.95
2012/07/10	12:49	36.83	138.39	9	5.2	108	43.80
2012/08/25	23:16	42.33	143.11	49	6.1	190	13.35
2012/09/14	02:22	35.86	140.54	37	5.1	98	52.48
2012/10/12	13:57	35.85	140.55	37	5.1	82	39.79

[a]Nsta: number of total recording stations regardless of source-station distance.

(Table 1). Finally, there are 2416 vertical-component seismic records with the hypocentral distances shorter than 100 km. The seismic records with the hypocentral distances shorter than 20 km are not used in this study to discard those consisting of near-source effect [*Yamada and Mori*, 2009].

3. Results and Discussion

Figure 2 shows the relation between 2416 pairs of P*d* and PGV. The resulting best fitting relationship between P*d* and PGV is given

$$\log(\mathrm{P}d) = 0.874\log(\mathrm{PGV}) - 1.139 \pm 0.177, \quad (1)$$

with the correlation coefficient of 0.85. The correlations between τ_c and the size of 123 earthquakes (M_{JMA}) are shown in Figure 3 with the hypocentral distances from (Figure 3a) 20 to 40 km and from (Figure 3b) 30 to 50 km, respectively. A certain degree of fluctuation between τ_c and M_{JMA} is presented indicating that it is not well applicable to use a single parameter τ_c to estimate the earthquake size. The scatter might attribute to the finite fault effect and the individual source rupturing properties. The event with the combination of the larger τ_c and P*d* indicating larger magnitude and PGV, respectively, most likely causes damage in and around the station area. Figure 4 shows the relationship between τ_c*P*d* and M_{JMA} with the hypocentral distances from (Figure 4a) 20 to 40 km and from (Figure 4b) 30 to 50 km, respectively. The

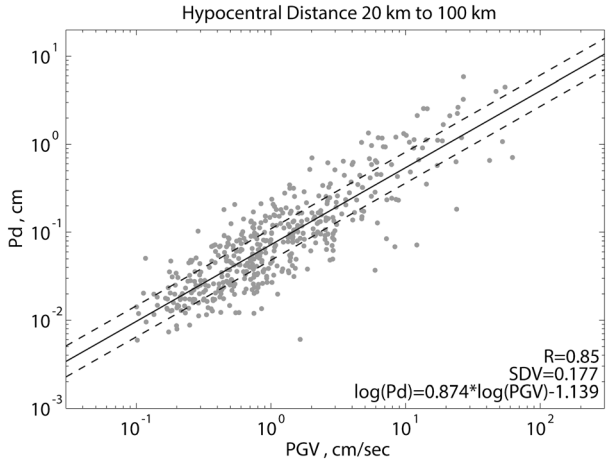

Figure 2. The relationship between P*d* and PGV at the hypocentral distances between 20 and 100 km.

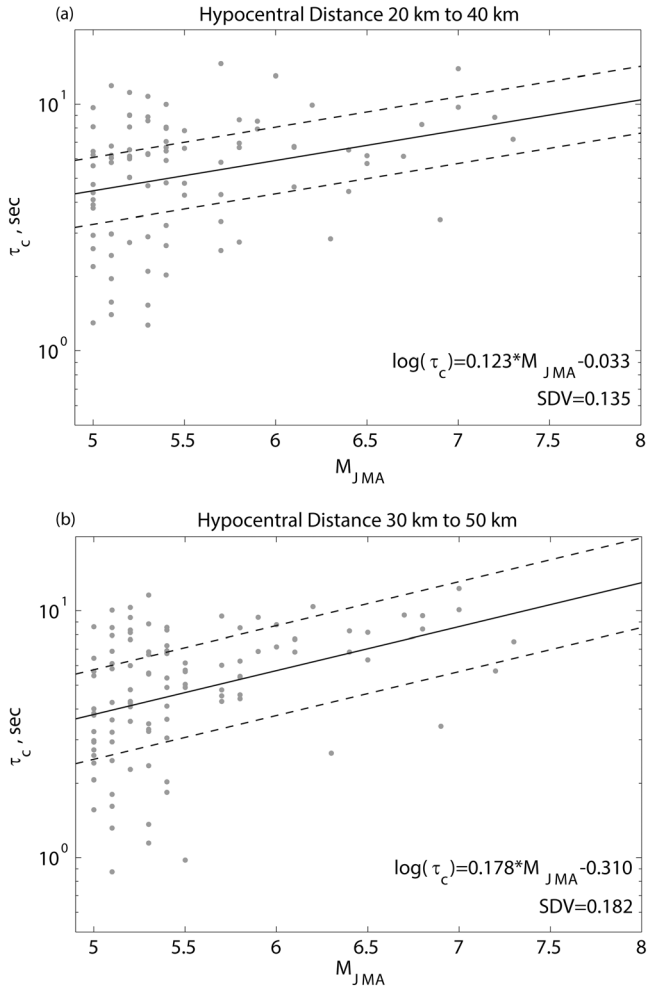

Figure 3. The average τ_c measurements for the 123 events versus M_{JMA} with the hypocentral distances ranging from (a) 20 to 40 km and (b) 30 to 50 km, respectively.

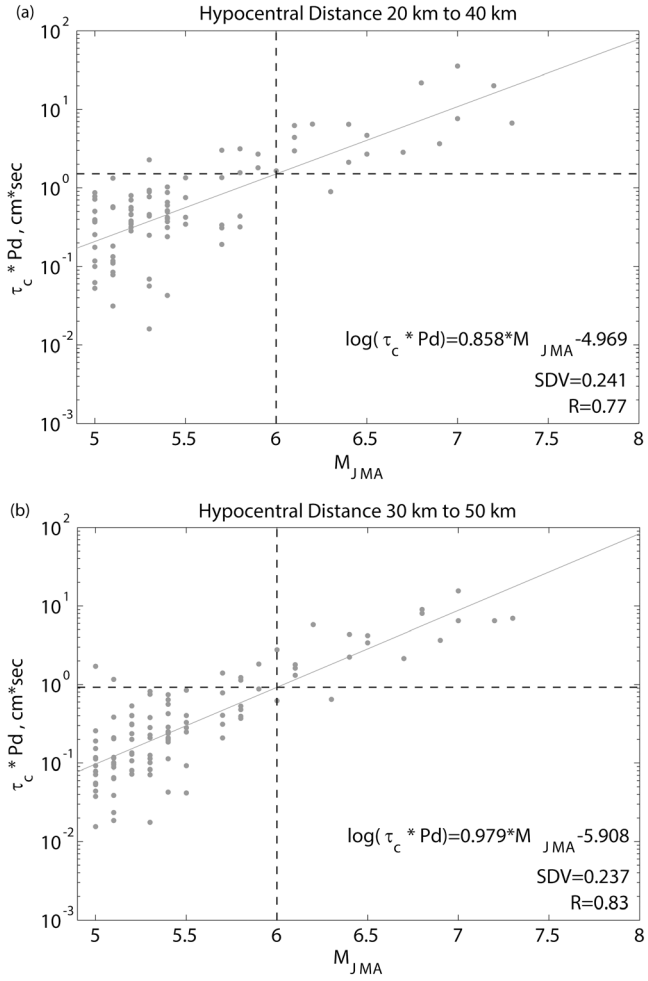

Figure 4. Relationship between average τ_c*Pd and M_{JMA} for the 123 events with the hypocentral distances ranging from (a) 20 to 40 km and (b) 30 to 50 km, respectively.

correlations between τ_c*Pd and M_{JMA} are noticeable with correlation coefficients of 0.77 and 0.83 for two hypocentral distance ranges, respectively. The respective best fit regressions are given

$$\log(\tau_c\text{*P}d) = 0.858\text{*}M_{JMA} - 4.969 \pm 0.241, \quad (2)$$

$$\log(\tau_c\text{*P}d) = 0.979\text{*}M_{JMA} - 5.908 \pm 0.237. \quad (3)$$

Figure 4a shows that 16 out of 17 (94%) events with $M_{JMA} \geq 6.0$ have the values of τ_c*Pd larger than 1.0 s cm and 16 out of 22 (73%) events with τ_c*P$d \geq 1.0$ s cm have $M_{JMA} \geq 6.0$. Figure 4b shows that 17 out of 19 (89%) events with $M_{JMA} \geq 6.0$ have the values of τ_c*Pd larger than 1.0 s cm and 17 out of 23 (74%) events with τ_c*P$d \geq 1.0$ s cm have $M_{JMA} \geq 6.0$. The value of τ_c*Pd has a better correlation with earthquake magnitude than τ_c itself. The value of τ_c*Pd could be used to estimate the new type of the size of earthquake that is, to some degree, related to the potential of earthquake damage. *Wu and Kanamori* [2005b] proposed that if a station has P$d > 0.5$ cm and $\tau_c > 1.0$ s, the event is most like a damaging event both in the station and a larger areas. Figures 5a and 5c show the distribution of τ_c and Pd with the hypocentral distance from 20 to 40 km and from 30 to 50 km, respectively. Figures 5b and 5d show the corresponding PGV in Figures 5a and 5c. The results in Figure 5 suggest that if a station registers P$d > 0.5$ cm and $\tau_c > 1.0$ s, the station will mostly have PGV at least larger than 5.0 cm/s and the majority of PGV are larger than 10.0 cm/s. According to the

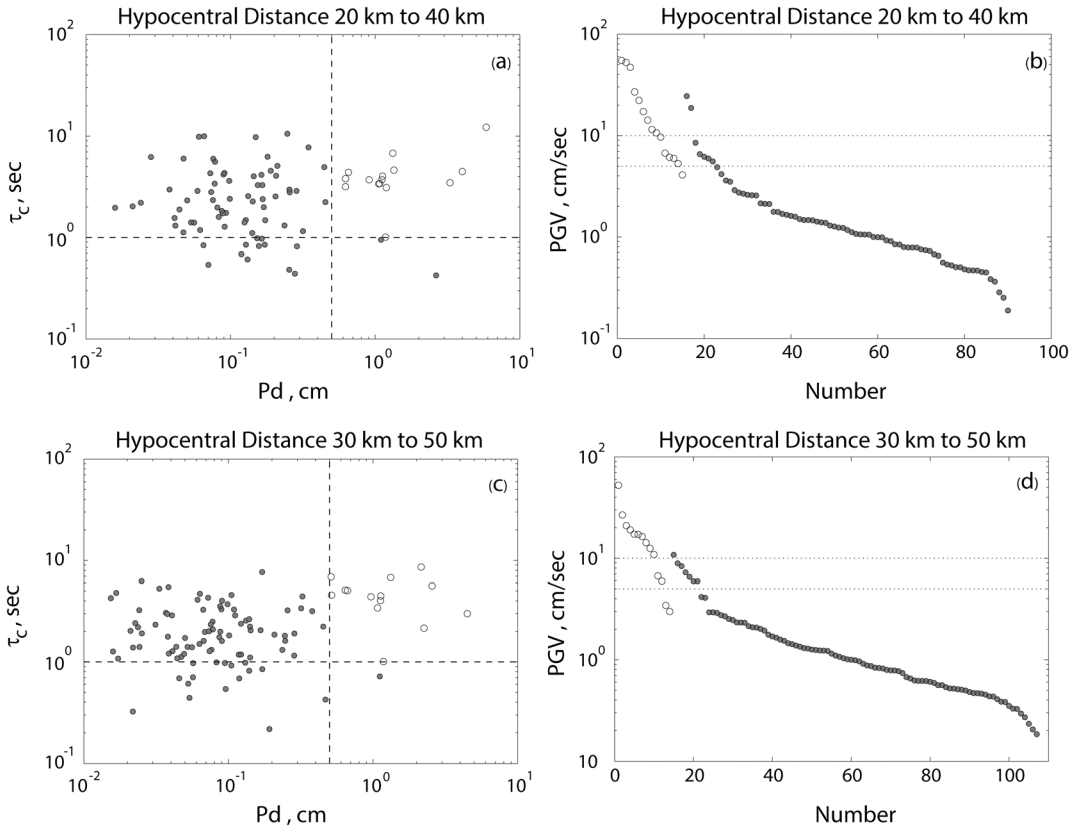

Figure 5. (a and c) The scatterplot of average τ_c and P*d* with the hypocentral distances ranging from 20 to 40 km and from 30 to 50 km, respectively. (b and d) The corresponding average PGV for the 123 events. $\tau_c > 1.0$ s and $Pd > 0.5$ cm are indicated by the open circles.

regression relationship between Modified Mercalli Intensity and PGV proposed by *Wald et al.* [1999], PGV of 5.0 and 10.0 cm/s are grouped in Intensity V (moderate shaking) and Intensity VI (strong shaking).

Acknowledgments

This research was supported by the Ministry of Science and Technology. The GMT software from *Wessel and Smith* [1998] was used in plotting part of the figures and is gratefully acknowledged. The waveform data are requested from KiK-net of National Research Institute for Earth Science and Disaster Prevention (NIED). We greatly appreciate NIED for providing data.

The Editor thanks Anthony Lomax and an anonymous reviewer for their assistance in evaluating this paper.

References

Alick, H., O. Ozel, Y. M. Wu, N. M. Ozel, and M. Erdik (2011), An alternative approach for the Istanbul earthquake early warning system, *Soil Dyn. Earthquake Eng.*, *31*, 181–187.

Allen, R. M., P. Gasparini, O. Kamigaichi, and M. Böse (2009), The status of earthquake early warning around the world: An introductory overview, *Seismol. Res. Lett.*, *80*, 682–693, doi:10.1785/gssrl.80.5.682.

Aoi, S., T. Kunugi, H. Nakamura, and H. Fujiwara (2011), Deployment of New Strong Motion Seismographs of K-NETK-NET and KiK-net, in *Earthquake Data in Engineering Seismology*, pp. 167–186, Springer, Netherlands.

Kanamori, H. (2005), Real-time seismology and earthquake damage mitigation, *Annu. Rev. Earth Planet. Sci.*, *33*, 195–214, doi:10.1146/annurev.earth.33.092203.122626.

Kanamori, H., E. Hauksson, and T. Heaton (1997), Real-time seismology and earthquake hazard mitigation, *Nature*, *390*, 461–464.

Lee, W. H. K., and Y. M. Wu (2009), Earthquake monitoring and early warning systems, in *Encyclopedia of Complexity and Systems Science*, vol. 11, edited by R. A. Meyers, 10,370 pp., Springer, New York.

Satriano, C., Y. M. Wu, A. Zollo, and H. Kanamori (2011), Earthquake early warning: Concepts, methods and physical grounds, *Soil Dyn. Earthquake Eng.*, *31*, 106–118, doi:10.1016/j.soildyn.2010.07.007.

Wald, D. J., V. Quitoriano, T. H. Heaton, and H. Kanamori (1999), Relationships between peak ground acceleration, peak ground velocity, and modified Mercalli intensity in California, *Earthquake Spectra*, *15*(3), 557–564.

Wessel, P., and W. H. F. Smith (1998), New improved version of Generic Mapping Tools released, *Eos Trans. AGU*, *79*, 579, doi:10.1029/98EO00426.

Wu, Y. M., and H. Kanamori (2005a), Experiment on an onsite early warning method for the Taiwan early warning system, *Bull. Seismol. Soc. Am.*, *95*, 347–353, doi:10.1785/0120040097.

Wu, Y. M., and H. Kanamori (2005b), Rapid assessment of damage potential of earthquakes in Taiwan from the beginning of P-waves, *Bull. Seismol. Soc. Am.*, *95*, 1181–1185, doi:10.1785/0120040193.

Wu, Y. M., and H. Kanamori (2008a), Development of an earthquake early warning system using real-time strong motion signals, *Sensors*, *8*, 1–9, doi:10.3390/s8010001.

Wu, Y. M., and H. Kanamori (2008b), Exploring the feasibility of on-site earthquake early warning using close-in records of the 2007 Noto Hanto earthquake, *Earth Planets Space*, *60*, 155–160.

Wu, Y. M., H. Kanamori, R. M. Allen, and E. Hauksson (2007), Determination of earthquake early warning parameters, τ_c and P*d*, for southern California, *Geophys. J. Int.*, *170*, 711–717, doi:10.1111/j.1365-246X.2007.03430.x.

Yamada, M., and J. Mori (2009), Using τ_c to estimate magnitude for earthquake early warning and effects of near-field terms, *J. Geophys. Res.*, *114*, B05301, doi:10.1029/2008JB006080.

Zollo, A., M. Lancieri, and S. Nielsen (2006), Earthquake magnitude estimation from peak amplitudes of very early seismic signals on strong motion records, *Geophys. Res. Lett.*, *33*, L23312, doi:10.1029/2006GL027795.

Zollo, A., O. Amoroso, M. Lancieri, Y.-M. Wu, and H. Kanamori (2010), A threshold-based earthquake early warning using dense accelerometer networks, *Geophys. J. Int.*, *183*, 963–974, doi:10.1111/j.1365-246X.2010.04765.x.